6

High-Resolution Methods

In Chapter 4 we developed the basic ideas of Godunov's method, an upwind finite volume method for hyperbolic systems, in the context of constant-coefficient linear systems. Godunov's method is only first-order accurate and introduces a great deal of numerical diffusion, yielding poor accuracy and smeared results, as can be seen in Figure 6.1(a), for example. In this chapter we will see how this method can be greatly improved by introducing correction terms into (4.43), to obtain a method of the form

$$Q_i^{n+1} = Q_i - \frac{\Delta t}{\Delta x}\left(A^+ \Delta Q_{i-1/2} + A^- \Delta Q_{i+1/2}\right) - \frac{\Delta t}{\Delta x}\left(\tilde{F}_{i+1/2} - \tilde{F}_{i-1/2}\right). \quad (6.1)$$

The fluxes $\tilde{F}_{i-1/2}$ are based on the waves resulting from the Riemann solution, which have already been computed in the process of determining the fluctuations $\mathcal{A}^{\pm}\Delta Q_{i-1/2}$. The basic form of these correction terms is motivated by the *Lax–Wendroff method*, a standard second-order accurate method described in the next section. The addition of crucial *limiters* leads to great improvement, as discussed later in this chapter.

6.1 The Lax–Wendroff Method

The Lax–Wendroff method for the linear system $q_t + Aq_x = 0$ is based on the Taylor series expansion

$$q(x, t_{n+1}) = q(x, t_n) + \Delta t\, q_t(x, t_n) + \frac{1}{2}(\Delta t)^2 q_{tt}(x, t_n) + \cdots. \quad (6.2)$$

From the differential equation we have that $q_t = -Aq_x$, and differentiating this gives

$$q_{tt} = -Aq_{xt} = A^2 q_{xx},$$

where we have used $q_{xt} = q_{tx} = (-Aq_x)_x$. Using these expressions for q_t and q_{tt} in (6.2) gives

$$q(x, t_{n+1}) = q(x, t_n) - \Delta t\, Aq_x(x, t_n) + \frac{1}{2}(\Delta t)^2 A^2 q_{xx}(x, t_n) + \cdots. \quad (6.3)$$

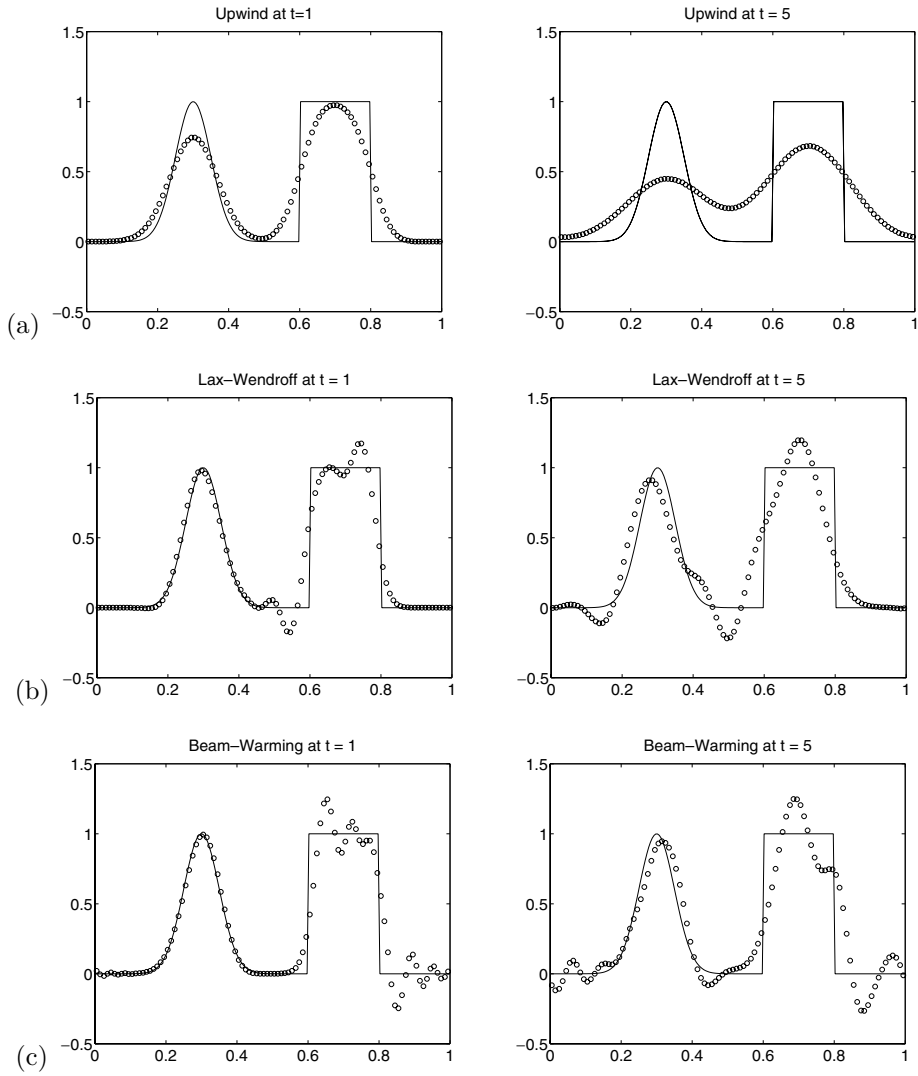

Fig. 6.1. Tests on the advection equation with different linear methods. Results at time $t = 1$ and $t = 5$ are shown, corresponding to 1 and 5 revolutions through the domain in which the equation $q_t + q_x = 0$ is solved with periodic boundary conditions: (a) upwind, (b) Lax–Wendroff, (c) Beam–Warming. `[claw/book/chap6/compareadv]`

Keeping only the first three terms on the right-hand side and replacing the spatial derivatives by central finite difference approximations gives the *Lax–Wendroff method*,

$$Q_i^{n+1} = Q_i^n - \frac{\Delta t}{2\,\Delta x} A\big(Q_{i+1}^n - Q_{i-1}^n\big) + \frac{1}{2}\left(\frac{\Delta t}{\Delta x}\right)^2 A^2\big(Q_{i-1}^n - 2Q_i^n + Q_{i+1}^n\big). \qquad (6.4)$$

By matching three terms in the Taylor series and using centered approximations, we obtain a second-order accurate method.

This derivation of the method is based on a finite difference interpretation, with Q_i^n approximating the pointwise value $q(x_i, t_n)$. However, we can reinterpret (6.4) as a finite

volume method of the form (4.4) with the flux function

$$F^n_{i-1/2} = \frac{1}{2}A\big(Q^n_{i-1} + Q^n_i\big) - \frac{1}{2}\frac{\Delta t}{\Delta x}A^2\big(Q^n_i - Q^n_{i-1}\big). \tag{6.5}$$

Note that this looks like the unstable averaged flux (4.18) plus a diffusive flux, but that the diffusion chosen exactly matches what appears in the Taylor series expansion (6.3). Indeed, this shows why the averaged flux (4.18) alone is unstable – the Taylor series expansion for the true solution contains a diffusive q_{xx} term that is missing from the numerical method when the unstable flux is used.

To compare the typical behavior of the upwind and Lax–Wendroff methods, Figure 6.1 shows numerical solutions to the scalar advection equation $q_t + q_x = 0$, which is solved on the unit interval up to time $t = 1$ with periodic boundary conditions. Hence the solution should agree with the initial data, translated back to the initial location. The data, shown as a solid line in each plot, consists of both a smooth pulse and a square-wave pulse. Figure 6.1(a) shows the results when the upwind method is used. Excessive dissipation of the solution is evident. Figure 6.1(b) shows the results when the Lax–Wendroff method is used instead. The smooth pulse is captured much better, but the square wave gives rise to an oscillatory solution. This can be explained in terms of the Taylor series expansion (6.2) as follows. By matching the first three terms in the series expansion, the dominant error is given by the next term, $q_{ttt} = -A^3 q_{xxx}$. This is a *dispersive* term, which leads to oscillations, as explained in more detail in Section 8.6 where modified equations are discussed. In this chapter we will see a different explanation of these oscillations, along with a cure based on limiters.

In each of these figures the results were computed using a Courant number $\Delta t/\Delta x = 0.8$. Choosing different values gives somewhat different results, though the same basic behavior. Each method works best when the Courant number is close to 1 (and in fact is *exact* if the Courant number is exactly 1 for this simple problem) and less well for smaller values of $\Delta t/\Delta x$. The reader is encouraged to experiment with the CLAWPACK codes in the directories referenced in the figures.

6.2 The Beam–Warming Method

The Lax–Wendroff method (6.4) is a centered three-point method. If we have a system for which all the eigenvalues of A are positive (e.g., the scalar advection equation with $\bar{u} > 0$), then we might think it is preferable to use a one-sided formula. In place of the centered formula for q_x and q_{xx}, we might use

$$\begin{aligned} q_x(x_i, t_n) &= \frac{1}{2\,\Delta x}[3q(x_i, t_n) - 4q(x_{i-1}, t_n) + q(x_{i-2}, t_n)] + \mathcal{O}(\Delta x^2), \\ q_{xx}(x_i, t_n) &= \frac{1}{(\Delta x)^2}[q(x_i, t_n) - 2q(x_{i-1}, t_n) + q(x_{i-2}, t_n)] + \mathcal{O}(\Delta x). \end{aligned} \tag{6.6}$$

Using these in (6.3) gives a method that is again second-order accurate,

$$Q^{n+1}_i = Q^n_i - \frac{\Delta t}{2\,\Delta x}A\big(3Q^n_i - 4Q^n_{i-1} + Q^n_{i-2}\big) + \frac{1}{2}\left(\frac{\Delta t}{\Delta x}\right)^2 A^2\big(Q^n_i - 2Q^n_{i-1} + Q^n_{i-2}\big). \tag{6.7}$$

This is known as the *Beam–Warming method*, and was originally introduced in [481]. It can be written as a flux-differencing finite volume method with

$$F^n_{i-1/2} = AQ^n_{i-1} + \frac{1}{2}A\left(1 - \frac{\Delta t}{\Delta x}A\right)\left(Q^n_{i-1} - Q^n_{i-2}\right). \tag{6.8}$$

Figure 6.1(c) shows the results of the previous advection test using the Beam–Warming method. The behavior is similar to that of the Lax–Wendroff method in that oscillations appear, though the oscillations are now ahead of the discontinuities rather than behind.

6.3 Preview of Limiters

Second-order accurate methods such as the Lax–Wendroff or Beam–Warming give much better accuracy on smooth solutions than the upwind method, as seen in Figure 6.1, but fail near discontinuities, where oscillations are generated. In fact, even when the solution is smooth, oscillations may appear due to the dispersive nature of these methods, as evident in Figure 6.1. Upwind methods have the advantage of keeping the solution monotonically varying in regions where the solution should be monotone, even though the accuracy is not very good. The idea with *high-resolution* methods is to combine the best features of both methods. Second-order accuracy is obtained where possible, but we don't insist on it in regions where the solution is not behaving smoothly (and the Taylor series expansion is not even valid). With this approach we can achieve results like those shown in Figure 6.2.

The dispersive nature of the Lax–Wendroff method also causes a slight shift in the location of the smooth hump, a *phase error*, that is visible in Figure 6.1, particularly at the later time $t = 5$. Another advantage of using limiters is that this phase error can be essentially eliminated. Figure 6.3 shows a computational example where the initial data consists of a *wave packet*, a high-frequency signal modulated by a Gaussian. With a dispersive method such a packet will typically propagate at an incorrect speed corresponding to the numerical *group velocity* of the method. The Lax–Wendroff method is clearly quite dispersive. The high-resolution method shown in Figure 6.3(c) performs much better. There is some dissipation of the wave, but much less than with the upwind method. The main goal of this chapter is to develop the class of high-resolution methods used to obtain these results.

A hint of how this can be done is seen by rewriting the Lax-Wendroff flux (6.5) as

$$F^n_{i-1/2} = \left(A^- Q^n_i + A^+ Q^n_{i-1}\right) + \frac{1}{2}|A|\left(I - \frac{\Delta t}{\Delta x}|A|\right)\left(Q^n_i - Q^n_{i-1}\right), \tag{6.9}$$

using the notation A^-, A^+, $|A|$ defined in Section 4.12. This now has the form of the upwind flux (4.56) with a correction term. Using this in the flux-differencing method (4.4) gives a method of the form (6.1). Note that the correction term in (6.9) looks like a diffusive flux, since it depends on $Q^n_i - Q^n_{i-1}$ and has the form of (4.10), but the coefficient is positive if the CFL condition is satisfied. Hence it corresponds to an *antidiffusive flux* that has the effect of sharpening up the overly diffusive upwind approximation.

The idea is now to modify the final term in (6.9) by applying some form of *limiter* that changes the magnitude of the correction actually used, depending on how the solution is behaving. The limiting process is complicated by the fact that the solution to a hyperbolic system typically consists of a superposition of waves in several different families. At a given

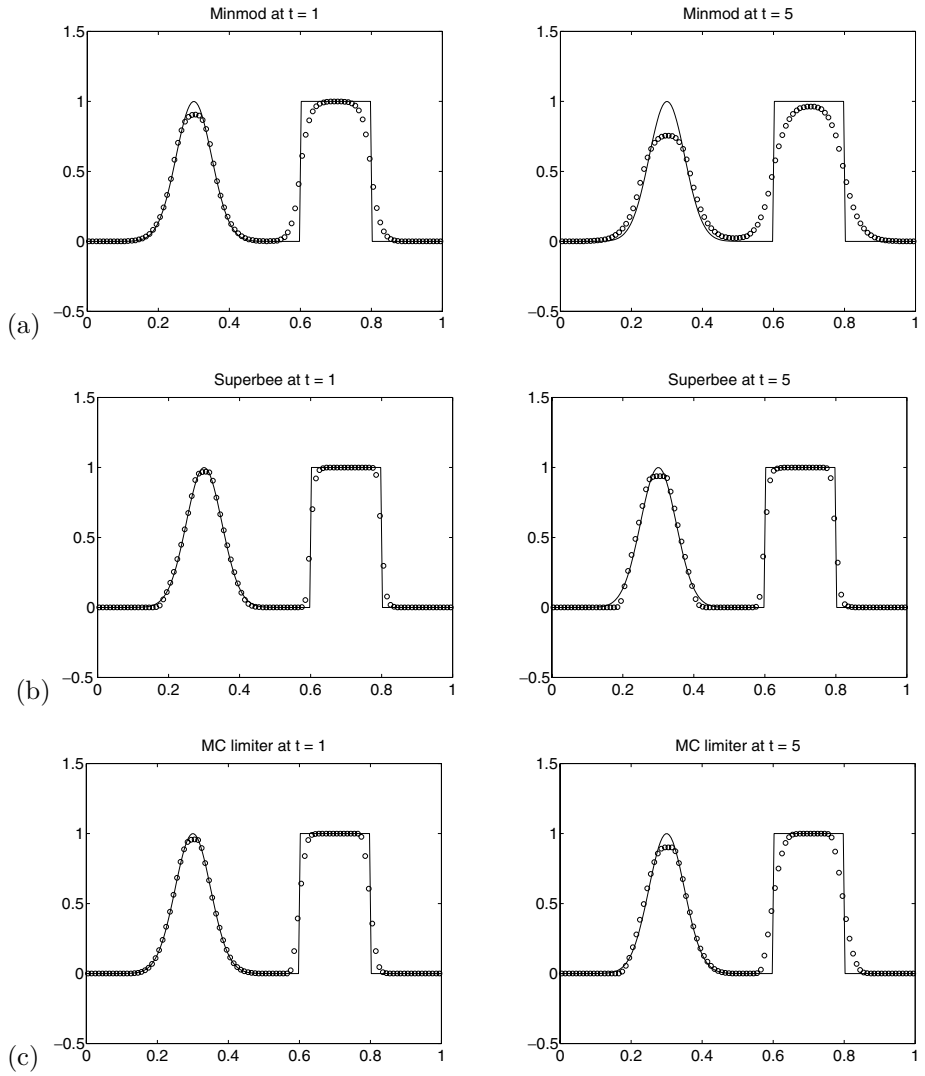

Fig. 6.2. Tests on the advection equation with different high-resolution methods, as in Figure 6.1: (a) minmod limiter, (b) superbee limiter, (c) MC limiter. `[claw/book/chap6/compareadv]`

point and time, some of the waves passing by may be smooth while others are discontinuous. Ideally we would like to apply the limiters in such a way that the discontinuous portion of the solution remains nonoscillatory while the smooth portion remains accurate. To do so we must use the characteristic structure of the solution. We will see that this is easily accomplished once we have solved the Riemann problem necessary to implement the upwind Godunov method. The second-order correction terms can be computed based on the waves arising in that Riemann solution, with each wave limited independently from the others. This process is fully described later in this chapter.

More generally, one can consider combining any low-order flux formula $\mathcal{F}_L(Q_{i-1}, Q_i)$ (such as the upwind flux) and any higher-order formula $\mathcal{F}_H(Q_{i-1}, Q_i)$ (such as the

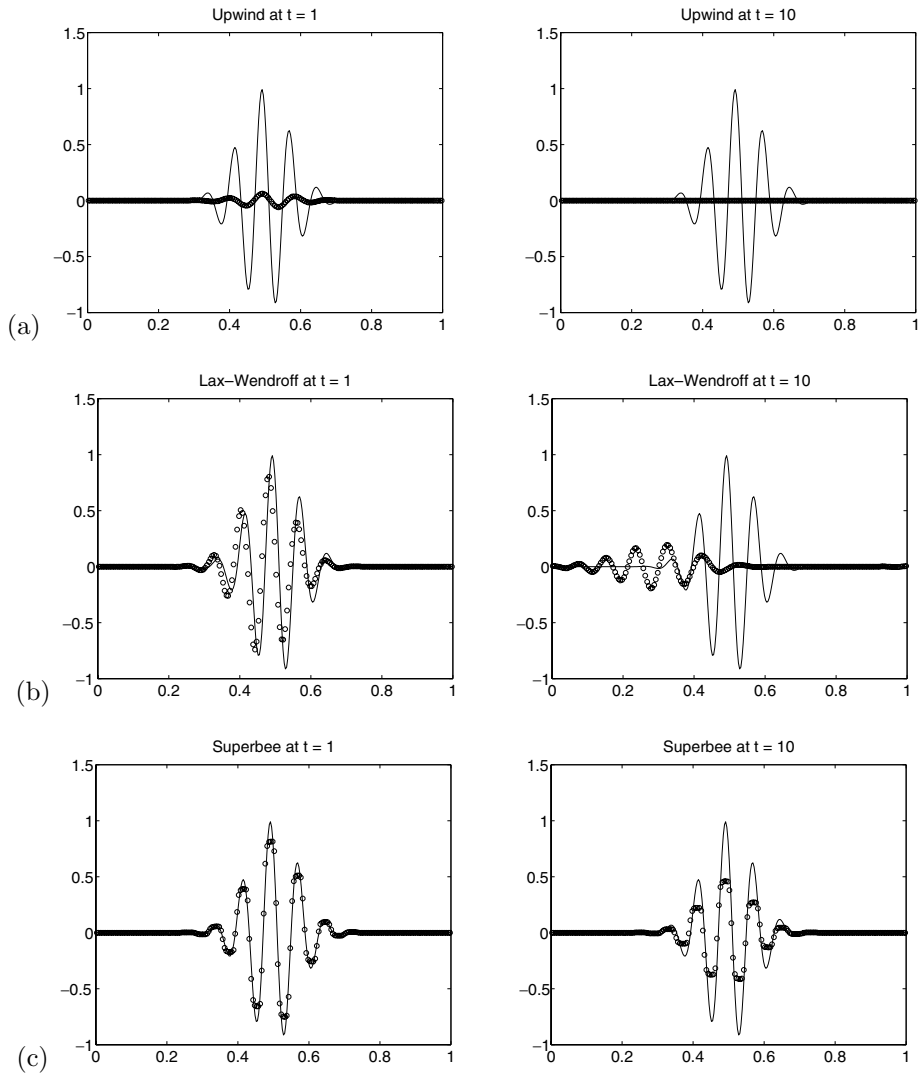

Fig. 6.3. Tests on the advection equation with different methods on a wave packet. Results at time $t = 1$ and $t = 10$ are shown, corresponding to 1 and 10 revolutions through the domain in which the equation $q_t + q_x = 0$ is solved with periodic boundary conditions. `[claw/book/chap6/wavepacket]`

Lax–Wendroff) to obtain a *flux-limiter* method with

$$F^n_{i-1/2} = \mathcal{F}_L(Q_{i-1}, Q_i) + \Phi^n_{i-1/2}[\mathcal{F}_H(Q_{i-1}, Q_i) - \mathcal{F}_L(Q_{i-1}, Q_i)]. \tag{6.10}$$

If $\Phi^n_{i-1/2} = 0$, then this reduces to the low-order method, while if $\Phi^n_{i-1/2} = 1$, we obtain the high-order method. This idea of applying limiters to improve the behavior of high-order methods appeared in the early 1970s in the *hybrid method* of Harten and Zwas [190] and the *flux-corrected transport* (FCT) method of Boris and Book [38] (see also [348], [496]). A wide variety of other methods of this form have since been developed, along with better

theoretical techniques to analyze them. In this chapter we combine many of these ideas to develop a class of methods that is relatively easy to extend to harder problems.

In the next section we start by giving a geometric interpretation for the scalar advection equation, leading to *slope-limiter* methods of the type pioneered in van Leer's work [464]–[468]. For the scalar advection equation there are many ways to interpret the same method, and it is illuminating to explore these. In particular we will see how this relates to flux-limiter methods of the type studied by Sweby [429], who used the algebraic total variation diminishing (TVD) conditions of Harten [179] to derive conditions that limiter functions should satisfy for more general nonlinear conservation laws. We will, however, ultimately use a different approach to apply these limiters to nonlinear problems, closer to the geometric approach in Goodman & LeVeque [160]. This can be interpreted as applying the limiter functions to the waves resulting from the Riemann solution. Extending this to linear systems of equations gives the algorithm introduced in Section 6.13. The method is then easily generalized to nonlinear systems, as described briefly in Section 6.15 and more fully in Chapter 15. Multidimensional versions are discussed in Chapters 19 through 23.

6.4 The REA Algorithm with Piecewise Linear Reconstruction

Recall the reconstruct–evolve–average (REA) Algorithm 4.1 introduced in Section 4.10. For the scalar advection equation we derived the upwind method by reconstructing a piecewise constant function $\tilde{q}^n(x, t_n)$ from the cell averages Q_i^n, solving the advection equation with this data, and averaging the result at time t_{n+1} over each grid cell to obtain Q_i^{n+1}. To achieve better than first-order accuracy, we must use a better reconstruction than a piecewise constant function. From the cell averages Q_i^n we can construct a piecewise linear function of the form

$$\tilde{q}^n(x, t_n) = Q_i^n + \sigma_i^n(x - x_i) \qquad \text{for } x_{i-1/2} \le x < x_{i+1/2}, \tag{6.11}$$

where

$$x_i = \frac{1}{2}\left(x_{i-1/2} + x_{i+1/2}\right) = x_{i-1/2} + \frac{1}{2}\Delta x \tag{6.12}$$

is the center of the ith grid cell and σ_i^n is the slope on the ith cell. The linear function (6.11) on the ith cell is defined in such a way that its value at the cell center x_i is Q_i^n. More importantly, the average value of $\tilde{q}^n(x, t_n)$ over cell $\mathcal{C}_i$ is Q_i^n (regardless of the slope σ_i^n), so that the reconstructed function has the cell average Q_i^n. This is crucial in developing conservative methods for conservation laws. Note that steps 2 and 3 are conservative in general, and so Algorithm 4.1 is conservative provided we use a *conservative reconstruction* in step 1, as we have in (6.11). Later we will see how to write such methods in the standard conservation form (4.4).

For the scalar advection equation $q_t + \bar{u}q_x = 0$, we can easily solve the equation with this data, and compute the new cell averages as required in step 3 of Algorithm 4.1. We have

$$\tilde{q}^n(x, t_{n+1}) = \tilde{q}^n(x - \bar{u}\,\Delta t, t_n).$$

Until further notice we will assume that $\bar{u} > 0$ and present the formulas for this particular case. The corresponding formulas for $\bar{u} < 0$ should be easy to derive, and in Section 6.10 we will see a better way to formulate the methods in the general case.

Suppose also that $|\bar{u}\,\Delta t/\Delta x| \le 1$, as is required by the CFL condition. Then it is straightforward to compute that

$$\begin{aligned} Q_i^{n+1} &= \frac{\bar{u}\,\Delta t}{\Delta x}\left(Q_{i-1}^n + \frac{1}{2}(\Delta x - \bar{u}\,\Delta t)\sigma_{i-1}^n\right) + \left(1 - \frac{\bar{u}\,\Delta t}{\Delta x}\right)\left(Q_i^n - \frac{1}{2}\bar{u}\,\Delta t\,\sigma_i^n\right) \\ &= Q_i^n - \frac{\bar{u}\,\Delta t}{\Delta x}\left(Q_i^n - Q_{i-1}^n\right) - \frac{1}{2}\frac{\bar{u}\,\Delta t}{\Delta x}\,(\Delta x - \bar{u}\,\Delta t)\left(\sigma_i^n - \sigma_{i-1}^n\right). \end{aligned} \tag{6.13}$$

Again note that this is the upwind method with a correction term that depends on the slopes.

6.5 Choice of Slopes

Choosing slopes $\sigma_i^n \equiv 0$ gives Godunov's method (the upwind method for the advection equation), since the final term in (6.13) drops out. To obtain a second-order accurate method we want to choose nonzero slopes in such a way that σ_i^n approximates the derivative q_x over the ith grid cell. Three obvious possibilities are

$$\text{Centered slope:} \qquad \sigma_i^n = \frac{Q_{i+1}^n - Q_{i-1}^n}{2\,\Delta x} \qquad \text{(Fromm)}, \tag{6.14}$$

$$\text{Upwind slope:} \qquad \sigma_i^n = \frac{Q_i^n - Q_{i-1}^n}{\Delta x} \qquad \text{(Beam–Warming)}, \tag{6.15}$$

$$\text{Downwind slope:} \qquad \sigma_i^n = \frac{Q_{i+1}^n - Q_i^n}{\Delta x} \qquad \text{(Lax–Wendroff)}. \tag{6.16}$$

The centered slope might seem like the most natural choice to obtain second-order accuracy, but in fact all three choices give the same formal order of accuracy, and it is the other two choices that give methods we have already derived using the Taylor series expansion. Only the downwind slope results in a centered three-point method, and this choice gives the Lax–Wendroff method. The upwind slope gives a fully-upwinded 3-point method, which is simply the Beam–Warming method.

The centered slope (6.14) may seem the most symmetric choice at first glance, but because the reconstructed function is then advected in the positive direction, the final updating formula turns out to be a nonsymmetric four-point formula,

$$\begin{aligned} Q_i^{n+1} = Q_i^n &- \frac{\bar{u}\,\Delta t}{4\,\Delta x}\left(Q_{i+1}^n + 3Q_i^n - 5Q_{i-1}^n + Q_{i-2}^n\right) \\ &- \frac{\bar{u}^2\,\Delta t^2}{4\,\Delta x^2}\left(Q_{i+1}^n - Q_i^n - Q_{i-1}^n + Q_{i-2}^n\right). \end{aligned} \tag{6.17}$$

This method is known as *Fromm's method*.

6.6 Oscillations

As we have seen in Figure 6.1, second-order methods such as the Lax–Wendroff or Beam–Warming (and also Fromm's method) give oscillatory approximations to discontinuous solutions. This can be easily understood using the interpretation of Algorithm 4.1.

Consider the Lax–Wendroff method, for example, applied to piecewise constant data with values

$$Q_i^n = \begin{cases} 1 & \text{if } i \le J, \\ 0 & \text{if } i > J. \end{cases}$$

Choosing slopes in each grid cell based on the Lax–Wendroff prescription (6.16) gives the piecewise linear function shown in Figure 6.4(a). The slope σ_i^n is nonzero only for $i = J$.

The function $\tilde{q}^n(x, t_n)$ has an *overshoot* with a maximum value of 1.5 regardless of Δx. When we advect this profile a distance $\bar{u}\,\Delta t$, and then compute the average over the Jth cell, we will get a value that is greater than 1 for any Δt with $0 < \bar{u}\,\Delta t < \Delta x$. The worst case is when $\bar{u}\,\Delta t = \Delta x/2$, in which case $\tilde{q}^n(x, t_{n+1})$ is shown in Figure 6.4(b) and $Q_J^{n+1} = 1.125$. In the next time step this overshoot will be accentuated, while in cell $J - 1$ we will now have a positive slope, leading to a value Q_{J-1}^{n+1} that is less than 1. This oscillation then grows with time.

The slopes proposed in the previous section were based on the assumption that the solution is smooth. Near a discontinuity there is no reason to believe that introducing this slope will improve the accuracy. On the contrary, if one of our goals is to avoid nonphysical oscillations, then in the above example we must set the slope to zero in the Jth cell. Any $\sigma_J^n < 0$ will lead to $Q_J^{n+1} > 1$, while a positive slope wouldn't make much sense. On the other hand we don't want to set all slopes to zero all the time, or we simply have the first-order upwind method. Where the solution is smooth we want second-order accuracy. Moreover, we will see below that even near a discontinuity, once the solution is somewhat smeared out over more than one cell, introducing nonzero slopes can help keep the solution from smearing out too far, and hence will significantly increase the resolution and keep discontinuities fairly sharp, as long as care is taken to avoid oscillations.

This suggests that we must pay attention to *how the solution is behaving* near the ith cell in choosing our formula for σ_i^n. (And hence the resulting updating formula will be nonlinear even for the linear advection equation). Where the solution is smooth, we want to choose something like the Lax–Wendroff slope. Near a discontinuity we may want to limit this slope, using a value that is smaller in magnitude in order to avoid oscillations. Methods based on this idea are known as *slope-limiter* methods. This approach was introduced by van

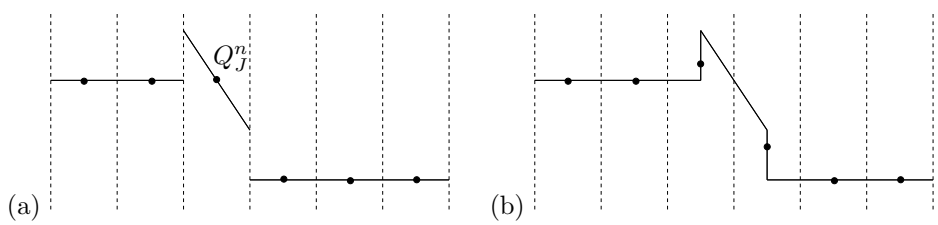

Fig. 6.4. (a) Grid values Q^n and reconstructed $\tilde{q}^n(\cdot, t_n)$ using Lax–Wendroff slopes. (b) After advection with $\bar{u}\,\Delta t = \Delta x/2$. The dots show the new cell averages Q^{n+1}. Note the overshoot.

Leer in a series of papers, [464] through [468], where he developed the approach known as *MUSCL* (monotonic upstream-centered scheme for conservation laws) for nonlinear conservation laws.

6.7 Total Variation

How much should we limit the slope? Ideally we would like to have a mathematical prescription that will allow us to use the Lax–Wendroff slope whenever possible, for second-order accuracy, while guaranteeing that no nonphysical oscillations will arise. To achieve this we need a way to measure oscillations in the solution. This is provided by the notion of the *total variation* of a function. For a grid function Q we define

$$\mathrm{TV}(Q) = \sum_{i=-\infty}^{\infty} |Q_i - Q_{i-1}|. \tag{6.18}$$

For an arbitrary function $q(x)$ we can define

$$\mathrm{TV}(q) = \sup \sum_{j=1}^{N} |q(\xi_j) - q(\xi_{j-1})|, \tag{6.19}$$

where the supremum is taken over all subdivisions of the real line $-\infty = \xi_0 < \xi_1 < \cdots < \xi_N = \infty$. Note that for the total variation to be finite, Q or q must approach constant values $q^{\pm}$ as $x \to \pm\infty$.

Another possible definition for functions is

$$\mathrm{TV}(q) = \limsup_{\epsilon \to 0} \frac{1}{\epsilon} \int_{-\infty}^{\infty} |q(x) - q(x-\epsilon)|\, dx. \tag{6.20}$$

If q is differentiable, then this reduces to

$$\mathrm{TV}(q) = \int_{-\infty}^{\infty} |q'(x)|\, dx. \tag{6.21}$$

We can use (6.21) also for nondifferentiable functions (distributions) if we interpret $q'(x)$ as the distribution derivative (which includes delta functions at points where q is discontinuous). Note that if we define a function $\tilde{q}(x)$ from a grid function Q using a piecewise constant approximation, then $\mathrm{TV}(\tilde{q}) = \mathrm{TV}(Q)$.

The true solution to the advection equation simply propagates at speed $\bar{u}$ with unchanged shape, so that the total variation $\mathrm{TV}(q(\cdot, t))$ must be constant in time. A numerical solution to the advection equation might not have constant total variation, however. If the method introduces oscillations, then we would expect the total variation of Q^n to *increase* with time. We can thus attempt to avoid oscillations by requiring that the method not increase the total variation:

Definition 6.1. *A two-level method is called* total variation diminishing (TVD) *if, for any set of data Q^n, the values Q^{n+1} computed by the method satisfy*

$$\mathrm{TV}(Q^{n+1}) \le \mathrm{TV}(Q^n). \tag{6.22}$$

Note that the total variation need not actually diminish in the sense of decreasing; it may remain constant in time. A better term might be *total variation nonincreasing*. In fact this term (and the abbreviation TVNI) was used in the original work of Harten [179], who introduced the use of this tool in developing and analyzing numerical methods for conservation laws. It was later changed to TVD as a less cumbersome term.

If a method is TVD, then in particular data that is initially monotone, say

$$Q_i^n \geq Q_{i+1}^n \qquad \text{for all } i,$$

will remain monotone in all future time steps. Hence if we discretize a single propagating discontinuity (as in Figure 6.4), the discontinuity may become smeared in future time steps but cannot become oscillatory. This property is especially useful, and we make the following definition.

Definition 6.2. *A method is called* monotonicity-preserving *if*

$$Q_i^n \geq Q_{i+1}^n \qquad \textit{for all } i$$

implies that

$$Q_i^{n+1} \geq Q_{i+1}^{n+1} \qquad \textit{for all } i.$$

Any TVD method is monotonicity-preserving; see Exercise 6.3.

6.8 TVD Methods Based on the REA Algorithm

How can we derive a method that is TVD? One easy way follows from the reconstruct–evolve–average approach to deriving methods described by Algorithm 4.1. Suppose that we perform the reconstruction in such a way that

$$\mathrm{TV}(\tilde{q}^n(\cdot, t_n)) \leq \mathrm{TV}(Q^n). \tag{6.23}$$

Then the method will be TVD. The reason is that the evolving and averaging steps cannot possibly increase the total variation, and so it is only the reconstruction that we need to worry about.

In the evolve step we clearly have

$$\mathrm{TV}(\tilde{q}^n(\cdot, t_{n+1})) = \mathrm{TV}(\tilde{q}^n(\cdot, t_n)) \tag{6.24}$$

for the advection equation, since $\tilde{q}^n$ simply advects without changing shape. The total variation turns out to be a very useful concept in studying nonlinear problems as well; for we will see later that a wide class of nonlinear scalar conservation laws also have this property, that the true solution has a nonincreasing total variation.

It is a simple exercise (Exercise 6.4) to show that the averaging step gives

$$\mathrm{TV}(Q^{n+1}) \leq \mathrm{TV}(\tilde{q}^n(\cdot, t_{n+1})). \tag{6.25}$$

Combining (6.23), (6.24), and (6.25) then shows that the method is TVD.

6.9 Slope-Limiter Methods

We now return to the derivation of numerical methods based on piecewise linear reconstruction, and consider how to limit the slopes so that (6.23) is satisfied. Note that setting $\sigma_i^n \equiv 0$ works, since the piecewise constant function has the same TV as the discrete data. Hence *the first-order upwind method is TVD* for the advection equation. The upwind method may smear solutions but cannot introduce oscillations.

One choice of slope that gives second-order accuracy for smooth solutions while still satisfying the TVD property is the *minmod slope*

$$\sigma_i^n = \text{minmod}\left(\frac{Q_i^n - Q_{i-1}^n}{\Delta x}, \frac{Q_{i+1}^n - Q_i^n}{\Delta x}\right), \tag{6.26}$$

where the minmod function of two arguments is defined by

$$\text{minmod}(a,b) = \begin{cases} a & \text{if } |a| < |b| \text{ and } ab > 0, \\ b & \text{if } |b| < |a| \text{ and } ab > 0, \\ 0 & \text{if } ab \le 0. \end{cases} \tag{6.27}$$

If a and b have the same sign, then this selects the one that is smaller in modulus, else it returns zero.

Rather than defining the slope on the ith cell by always using the downwind difference (which would give the Lax–Wendroff method), or by always using the upwind difference (which would give the Beam–Warming method), the minmod method compares the two slopes and chooses the one that is smaller in magnitude. If the two slopes have different sign, then the value Q_i^n must be a local maximum or minimum, and it is easy to check in this case that we must set $\sigma_i^n = 0$ in order to satisfy (6.23).

Figure 6.2(a) shows results using the minmod method for the advection problem considered previously. We see that the minmod method does a fairly good job of maintaining good accuracy in the smooth hump and also sharp discontinuities in the square wave, with no oscillations.

Sharper resolution of discontinuities can be achieved with other limiters that do not reduce the slope as severely as minmod near a discontinuity. Figure 6.5(a) shows some sample data representing a discontinuity smeared over two cells, along with the minmod slopes. Figure 6.5(b) shows that we can increase the slopes in these two cells to *twice* the value of the minmod slopes and still have (6.23) satisfied. This sharper reconstruction will lead to sharper resolution of the discontinuity in the next time step than we would obtain with the minmod slopes.

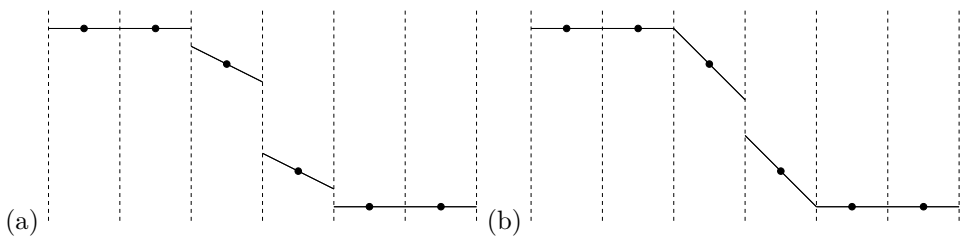

Fig. 6.5. Grid values Q^n and reconstructed $\tilde{q}^n(\cdot, t_n)$ using (a) minmod slopes, (b) superbee or MC slopes. Note that these steeper slopes can be used and still have the TVD property.

One choice of limiter that gives the reconstruction of Figure 6.5(b), while still giving second order accuracy for smooth solutions, is the so-called *superbee limiter* introduced by Roe [378]:

$$\sigma_i^n = \text{maxmod}\big(\sigma_i^{(1)}, \sigma_i^{(2)}\big), \tag{6.28}$$

where

$$\sigma_i^{(1)} = \text{minmod}\left(\left(\frac{Q_{i+1}^n - Q_i^n}{\Delta x}\right),\ 2\left(\frac{Q_i^n - Q_{i-1}^n}{\Delta x}\right)\right),$$
$$\sigma_i^{(2)} = \text{minmod}\left(2\left(\frac{Q_{i+1}^n - Q_i^n}{\Delta x}\right),\ \left(\frac{Q_i^n - Q_{i-1}^n}{\Delta x}\right)\right).$$

Each one-sided slope is compared with *twice* the opposite one-sided slope. Then the maxmod function in (6.28) selects the argument with *larger* modulus. In regions where the solution is smooth this will tend to return the *larger* of the two one-sided slopes, but will still be giving an approximation to q_x, and hence we expect second-order accuracy. We will see later that the superbee limiter is also TVD in general.

Figure 6.2(b) shows the same test problem as before but with the superbee method. The discontinuity stays considerably sharper. On the other hand, we see a tendency of the smooth hump to become steeper and squared off. This is sometimes a problem with superbee – by choosing the larger of the neighboring slopes it tends to steepen smooth transitions near inflection points.

Another popular choice is the *monotonized central-difference limiter* (MC limiter), which was proposed by van Leer [467]:

$$\sigma_i^n = \text{minmod}\left(\left(\frac{Q_{i+1}^n - Q_{i-1}^n}{2\Delta x}\right),\ 2\left(\frac{Q_i^n - Q_{i-1}^n}{\Delta x}\right),\ 2\left(\frac{Q_{i+1}^n - Q_i^n}{\Delta x}\right)\right). \tag{6.29}$$

This compares the central difference of Fromm's method with *twice* the one-sided slope to either side. In smooth regions this reduces to the centered slope of Fromm's method and hence does not tend to artificially steepen smooth slopes to the extent that superbee does. Numerical results with this limiter are shown in Figure 6.2(c). The MC limiter appears to be a good default choice for a wide class of problems.

6.10 Flux Formulation with Piecewise Linear Reconstruction

The slope-limiter methods described above can be written as flux-differencing methods of the form (4.4). The updating formulas derived above can be manipulated algebraically to determine what the numerical flux function must be. Alternatively, we can derive the numerical flux by computing the exact flux through the interface $x_{i-1/2}$ using the piecewise linear solution $\tilde{q}^n(x,t)$, by integrating $\bar{u}\tilde{q}^n(x_{i-1/2},t)$ in time from t_n to t_{n+1}. For the advection

equation this is easy to do and we find that

$$\begin{aligned} F^n_{i-1/2} &= \frac{1}{\Delta t}\int_{t_n}^{t_{n+1}} \bar{u}\tilde{q}^n\big(x_{i-1/2}, t\big)\,dt \\ &= \frac{1}{\Delta t}\int_{t_n}^{t_{n+1}} \bar{u}\tilde{q}^n\big(x_{i-1/2} - \bar{u}(t-t_n), t_n\big)\,dt \\ &= \frac{1}{\Delta t}\int_{t_n}^{t_{n+1}} \bar{u}\big[Q^n_{i-1} + \big(x_{i-1/2} - \bar{u}(t-t_n) - x_{i-1}\big)\sigma^n_{i-1}\big]dt \\ &= \bar{u}\,Q^n_{i-1} + \frac{1}{2}\bar{u}(\Delta x - \bar{u}\,\Delta t)\sigma^n_{i-1}. \end{aligned}$$

Using this in the flux-differencing formula (4.4) gives

$$Q^{n+1}_i = Q^n_i - \frac{\bar{u}\,\Delta t}{\Delta x}\big(Q^n_i - Q^n_{i-1}\big) - \frac{1}{2}\frac{\bar{u}\,\Delta t}{\Delta x}(\Delta x - \bar{u}\,\Delta t)\big(\sigma^n_i - \sigma^n_{i-1}\big),$$

which agrees with (6.13).

If we also consider the case $\bar{u} < 0$, then we will find that in general the numerical flux for a slope-limiter method is

$$F^n_{i-1/2} = \begin{cases} \bar{u}\,Q^n_{i-1} + \frac{1}{2}\bar{u}(\Delta x - \bar{u}\,\Delta t)\sigma^n_{i-1} & \text{if } \bar{u} \ge 0, \\ \bar{u}\,Q^n_i - \frac{1}{2}\bar{u}(\Delta x + \bar{u}\,\Delta t)\sigma^n_i & \text{if } \bar{u} \le 0, \end{cases} \tag{6.30}$$

where σ^n_i is the slope in the ith cell $\mathcal{C}_i$, chosen by one of the formulas discussed previously.

Rather than associating a slope σ^n_i with the ith cell, the idea of writing the method in terms of fluxes between cells suggests that we should instead associate our approximation to q_x with the cell interface at $x_{i-1/2}$ where $F^n_{i-1/2}$ is defined. Across the interface $x_{i-1/2}$ we have a jump

$$\Delta Q^n_{i-1/2} = Q^n_i - Q^n_{i-1}, \tag{6.31}$$

and this jump divided by Δx gives an approximation to q_x. This suggests that we write the flux (6.30) as

$$F^n_{i-1/2} = \bar{u}^- Q^n_i + \bar{u}^+ Q^n_{i-1} + \frac{1}{2}|\bar{u}|\left(1 - \left|\frac{\bar{u}\,\Delta t}{\Delta x}\right|\right)\delta^n_{i-1/2}, \tag{6.32}$$

where

$$\delta^n_{i-1/2} = \text{a limited version of } \Delta Q^n_{i-1/2}. \tag{6.33}$$

If $\delta^n_{i-1/2}$ is the jump $\Delta Q^n_{i-1/2}$ itself, then (6.32) gives the Lax–Wendroff method (see Exercise 6.6). From the form (6.32), we see that the Lax–Wendroff flux can be interpreted as a modification to the upwind flux (4.33). By limiting this modification we obtain a different form of the high-resolution methods, as explored in the next section.

6.11 Flux Limiters

From the above discussion it is natural to view the Lax–Wendroff method as the basic second-order method based on piecewise linear reconstruction, since defining the jump $\delta^n_{i-1/2}$ in (6.33) in the most obvious way as $\Delta Q^n_{i-1/2}$ at the interface $x_{i-1/2}$ results in that method. Other second-order methods have fluxes of the form (6.32) with different choices of $\delta^n_{i-1/2}$. The slope-limiter methods can then be reinterpreted as *flux-limiter methods* by choosing $\delta^n_{i-1/2}$ to be a limited version of (6.31). In general we will set

$$\delta^n_{i-1/2} = \phi\big(\theta^n_{i-1/2}\big)\Delta Q^n_{i-1/2}, \tag{6.34}$$

where

$$\theta^n_{i-1/2} = \frac{\Delta Q^n_{I-1/2}}{\Delta Q^n_{i-1/2}}. \tag{6.35}$$

The index I here is used to represent the interface on the *upwind* side of $x_{i-1/2}$:

$$I = \begin{cases} i-1 & \text{if } \bar{u} > 0, \\ i+1 & \text{if } \bar{u} < 0. \end{cases} \tag{6.36}$$

The ratio $\theta^n_{i-1/2}$ can be thought of as a measure of the smoothness of the data near $x_{i-1/2}$. Where the data is smooth we expect $\theta^n_{i-1/2} \approx 1$ (except at extrema). Near a discontinuity we expect that $\theta^n_{i-1/2}$ may be far from 1.

The function $\phi(\theta)$ is the *flux-limiter function*, whose value depends on the smoothness. Setting $\phi(\theta) \equiv 1$ for all θ gives the Lax–Wendroff method, while setting $\phi(\theta) \equiv 0$ gives upwind. More generally we might want to devise a limiter function ϕ that has values near 1 for $\theta \approx 1$, but that reduces (or perhaps increases) the slope where the data is not smooth.

There are many other ways one might choose to measure the smoothness of the data besides the variable θ defined in (6.35). However, the framework proposed above results in very simple formulas for the function ϕ corresponding to many standard methods, including all the methods discussed so far.

In particular, note the nice feature that choosing

$$\phi(\theta) = \theta \tag{6.37}$$

results in (6.34) becoming

$$\delta^n_{i-1/2} = \left(\frac{\Delta Q^n_{I-1/2}}{\Delta Q^n_{i-1/2}}\right)\Delta Q^n_{i-1/2} = \Delta Q^n_{I-1/2}.$$

Hence this choice results in the jump at the interface *upwind* from $x_{i-1/2}$ being used to define $\delta^n_{i-1/2}$ instead of the jump at this interface. As a result, the method (6.32) with the choice of limiter (6.37) reduces to the Beam–Warming method.

Since the centered difference (6.14) is the average of the one-sided slopes (6.15) and (6.16), we also find that Fromm's method can be obtained by choosing

$$\phi(\theta) = \frac{1}{2}(1+\theta). \tag{6.38}$$

Also note that $\phi(\theta) = 2$ corresponds to using $\delta^n_{i-1/2} = 2\,\Delta Q^n_{i-1/2}$, i.e., twice the jump at this interface, while $\phi(\theta) = 2\theta$ results in using twice the jump at the upwind interface. Recall that these are necessary ingredients in some of the slope limiters discussed in Section 6.9. Translating the various slope limiters into flux-limiter functions, we obtain the functions found below for the methods previously introduced.

Linear methods:

$$\begin{aligned} \text{upwind}: &\quad \phi(\theta) = 0, \\ \text{Lax–Wendroff}: &\quad \phi(\theta) = 1, \\ \text{Beam–Warming}: &\quad \phi(\theta) = \theta, \\ \text{Fromm}: &\quad \phi(\theta) = \frac{1}{2}(1+\theta). \end{aligned} \tag{6.39a}$$

High-resolution limiters:

$$\begin{aligned} \text{minmod}: &\quad \phi(\theta) = \text{minmod}(1,\theta), \\ \text{superbee}: &\quad \phi(\theta) = \max(0, \min(1, 2\theta), \min(2, \theta)), \\ \text{MC}: &\quad \phi(\theta) = \max(0, \min((1+\theta)/2, 2, 2\theta)) \\ \text{van Leer}: &\quad \phi(\theta) = \frac{\theta + |\theta|}{1 + |\theta|}. \end{aligned} \tag{6.39b}$$

The van Leer limiter listed here was proposed in [465]. A wide variety of other limiters have also been proposed in the literature. Many of these limiters are built into CLAWPACK. The parameter `mthlim` in `claw1ez` (see Section 5.4.6) determines which limiter is used. Other limiters are easily added to the code by modifying the file `claw/clawpack/1d/lib/philim.f`.

The flux-limiter method has the flux (6.32) with $\delta^n_{i-1/2}$ given by (6.34). Let $\nu = \bar{u}\,\Delta t/\Delta x$ be the Courant number. Then the flux-limiter method takes the form

$$\begin{aligned} Q^{n+1}_i = Q^n_i &- \nu\big(Q^n_i - Q^n_{i-1}\big) \\ &- \frac{1}{2}\nu(1-\nu)\big[\phi\big(\theta^n_{i+1/2}\big)\big(Q^n_{i+1} - Q^n_i\big) - \phi\big(\theta^n_{i-1/2}\big)\big(Q^n_i - Q^n_{i-1}\big)\big] \end{aligned} \tag{6.40}$$

if $\bar{u} > 0$, or

$$\begin{aligned} Q^{n+1}_i = Q^n_i &- \nu\big(Q^n_{i+1} - Q^n_i\big) \\ &+ \frac{1}{2}\nu(1+\nu)\big[\phi\big(\theta^n_{i+1/2}\big)\big(Q^n_{i+1} - Q^n_i\big) - \phi\big(\theta^n_{i-1/2}\big)\big(Q^n_i - Q^n_{i-1}\big)\big] \end{aligned} \tag{6.41}$$

if $\bar{u} < 0$.

6.12 TVD Limiters

For simple limiters such as minmod, it is clear from the derivation as a slope limiter (Section 6.9) that the resulting method is TVD, since it is easy to check that (6.23) is satisfied. For more complicated limiters we would like to have an algebraic proof that the

resulting method is TVD. A fundamental tool in this direction is the following theorem of Harten [179], which can be used to derive explicit algebraic conditions on the function ϕ required for a TVD method. For some other discussions of TVD conditions, see [180], [349], [429], [435], [465].

Theorem 6.1 (Harten). *Consider a general method of the form*

$$Q_i^{n+1} = Q_i^n - C_{i-1}^n\big(Q_i^n - Q_{i-1}^n\big) + D_i^n\big(Q_{i+1}^n - Q_i^n\big) \tag{6.42}$$

over one time step, where the coefficients C_{i-1}^n and D_i^n are arbitrary values (which in particular may depend on values of Q^n in some way, i.e., the method may be nonlinear). Then

$$\mathrm{TV}(Q^{n+1}) \le \mathrm{TV}(Q^n)$$

provided the following conditions are satisfied:

$$\begin{aligned} C_{i-1}^n &\ge 0 \quad \forall i, \\ D_i^n &\ge 0 \quad \forall i, \\ C_i^n + D_i^n &\le 1 \quad \forall i. \end{aligned} \tag{6.43}$$

Note: the updating formula for Q_i^{n+1} uses C_{i-1}^n and D_i^n, but the last condition involves C_i^n and D_i^n.

For the proof see Exercise 8.5. We can apply this theorem to the flux-limiter method for $q_t + \bar{u}q_x = 0$. We consider the case $\bar{u} > 0$ here (see Exercise 6.7 for the case $\bar{u} < 0$), so that the method has the form (6.40). There are many ways to rewrite this in the form (6.42), since C_{i-1}^n and D_i^n are allowed to depend on Q^n. The obvious choice is

$$\begin{aligned} C_{i-1}^n &= \nu - \frac{1}{2}\nu(1-\nu)\phi\big(\theta_{i-1/2}^n\big), \\ D_i^n &= -\frac{1}{2}\nu(1-\nu)\phi\big(\theta_{i+1/2}^n\big), \end{aligned}$$

but this can't be effectively used to prove the method is TVD, as there is no hope of satisfying the condition (6.43) using this. If $0 \le \nu \le 1$ then $D_i^n < 0$ when ϕ is near 1.

Instead note that

$$Q_{i+1}^n - Q_i^n = \big(Q_i^n - Q_{i-1}^n\big)/\theta_{i+1/2}^n,$$

and so the formula (6.40) can be put into the form (6.42) with

$$\begin{aligned} C_{i-1}^n &= \nu + \frac{1}{2}\nu(1-\nu)\left(\frac{\phi\big(\theta_{i+1/2}^n\big)}{\theta_{i+1/2}^n} - \phi\big(\theta_{i-1/2}^n\big)\right), \\ D_i^n &= 0. \end{aligned}$$

The conditions (6.43) are then satisfied provided that

$$0 \le C_{i-1}^n \le 1.$$

This in turn holds provided that the CFL condition $0 \le \nu \le 1$ holds, along with the bound

$$\left| \frac{\phi(\theta_1)}{\theta_1} - \phi(\theta_2) \right| \le 2 \qquad \text{for all values of } \theta_1, \theta_2. \tag{6.44}$$

If $\theta \le 0$, then we are at an extremum, and we know from our previous discussion that we should take $\phi(\theta) = 0$ in this case to achieve a TVD method. Also, when $\theta > 0$ we want $\phi(\theta) > 0$, since it generally doesn't make sense to negate the sign of the slope in applying the limiter. Since θ_1 and θ_2 in (6.44) are independent, we then see that we must require

$$0 \le \frac{\phi(\theta)}{\theta} \le 2 \quad \text{and} \quad 0 \le \phi(\theta) \le 2 \tag{6.45}$$

for all values of $\theta \ge 0$ in order to guarantee that condition (6.44) is satisfied (along with $\phi(\theta) = 0$ for $\theta < 0$). These constraints can be rewritten concisely as

$$0 \le \phi(\theta) \le \text{minmod}(2, 2\theta). \tag{6.46}$$

This defines the *TVD region* in the θ–ϕ plane: the curve $\phi(\theta)$ must lie in this region, which is shown as the shaded region in Figure 6.6(a). This figure also shows the functions $\phi(\theta)$

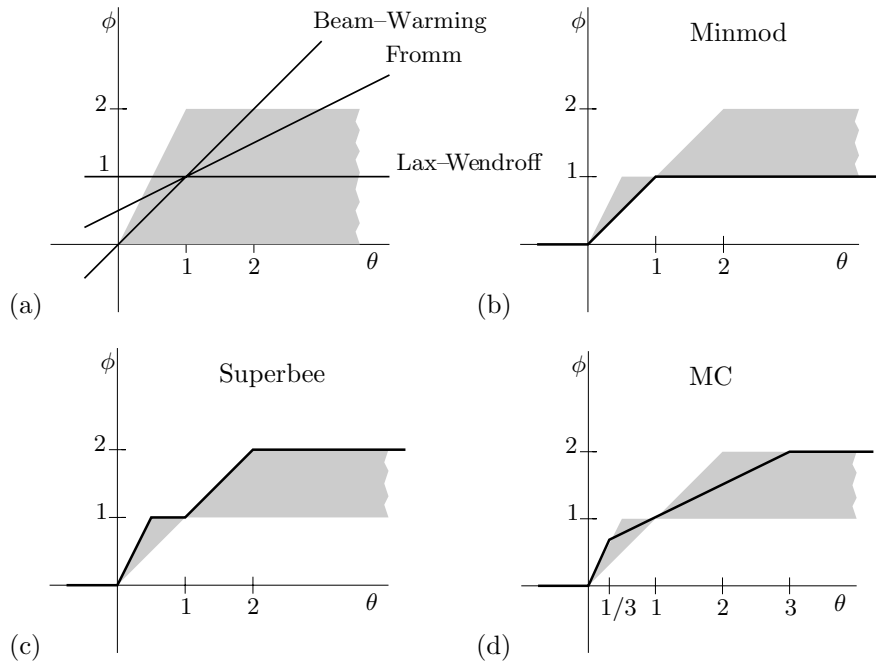

Fig. 6.6. Limiter functions $\phi(\theta)$. (a) The shaded regions shows where function values must lie for the method to be TVD. The second-order linear methods have functions $\phi(\theta)$ that leave this region. (b) The shaded region is the Sweby region of second-order TVD methods. The minmod limiter lies along the lower boundary. (c) The superbee limiter lies along the upper boundary. (d) The MC limiter is smooth at $\phi = 1$.

from (6.39a) for the Lax–Wendroff, Beam–Warming, and Fromm methods. All of these functions lie outside the shaded region for some values of θ, and indeed these methods are not TVD. This graphical analysis of ϕ was first presented by Sweby [429], who analyzed a wide class of flux-limiter methods (for nonlinear conservation laws as well as the advection equation).

Note that for any second-order accurate method we must have $\phi(1) = 1$. Sweby found, moreover, that it is best to take ϕ to be a convex combination of $\phi = 1$ (Lax–Wendroff) and $\phi = \theta$ (Beam–Warming). Other choices apparently give too much compression, and smooth data such as a sine wave tends to turn into a square wave as time evolves, as is already seen to happen with the superbee limiter. Imposing this additional restriction gives the second-order TVD region of Sweby, which is shown in Figure 6.6(b).

The high-resolution limiter functions from (6.39b) are all seen to satisfy the constraints (6.46), and these limiters all give TVD methods. The functions ϕ are graphed in Figure 6.6. Note that minmod lies along the lower boundary of the Sweby region, while superbee lies along the upper boundary. The fact that these functions are not smooth at $\theta = 1$ corresponds to the fact that there is a switch in the choice of one-sided approximation used as θ crosses this point. For full second-order accuracy we would like the function ϕ to be smooth near $\theta = 1$, as for the MC limiter. The van Leer limiter is an even smoother version of this.

We also generally want to impose a symmetry condition on the function $\phi(\theta)$. If the data Q^n is symmetric in x, then we might expect the reconstructed piecewise linear function to have this same property. It can be shown (Exercise 6.8) that this requires that the function ϕ also satisfy

$$\phi(1/\theta) = \frac{\phi(\theta)}{\theta}. \tag{6.47}$$

All of the high-resolution functions listed in (6.39b) satisfy this condition.

6.13 High-Resolution Methods for Systems

The slope-limiter or flux-limiter methods can also be extended to systems of equations. This is most easily done in the flux-limiter framework. First recall that the Lax–Wendroff method (6.4) can be written in flux-differencing form (4.4) if we define the flux by

$$\mathcal{F}(Q_{i-1}, Q_i) = \frac{1}{2}A(Q_{i-1} + Q_i) - \frac{1}{2}\frac{\Delta t}{\Delta x}A^2(Q_i - Q_{i-1}). \tag{6.48}$$

Since $A = A^+ + A^-$, we can rewrite this as

$$\mathcal{F}(Q_{i-1}, Q_i) = (A^+ Q_{i-1} + A^- Q_i) + \frac{1}{2}|A|\left(I - \frac{\Delta t}{\Delta x}|A|\right)(Q_i - Q_{i-1}), \tag{6.49}$$

where $|A| = A^+ - A^-$.

In the form (6.49), we see that the Lax–Wendroff flux can be viewed as being composed of the upwind flux (4.56) plus a correction term, just as for the scalar advection equation. To define a flux-limiter method we must limit the magnitude of this correction term according to how the data is varying. But for a system of equations, $\Delta Q_{i-1/2} = Q_i - Q_{i-1}$ is a vector, and it is not so clear how to compare this vector with the neighboring jump vector $\Delta Q_{i-3/2}$

or $\Delta Q_{i+1/2}$ to generalize (6.34). It is also not clear which neighboring jump to consider, since the "upwind" direction is different for each eigencomponent. The solution, of course, is that we must decompose the correction term in (6.49) into eigencomponents and limit each scalar eigencoefficient separately, based on the algorithm for scalar advection.

We can rewrite the correction term as

$$\frac{1}{2}|A|\left(I - \frac{\Delta t}{\Delta x}|A|\right)(Q_i - Q_{i-1}) = \frac{1}{2}|A|\left(I - \frac{\Delta t}{\Delta x}|A|\right)\sum_{p=1}^{m}\alpha_{i-1/2}^p r^p,$$

where r^p are the eigenvectors of A and the coefficients $\alpha_{i-1/2}^p$ are defined by (4.38). The flux-limiter method is defined by replacing the scalar coefficient $\alpha_{i-1/2}^p$ by a limited version, based on the scalar formulas of Section 6.11. We set

$$\tilde{\alpha}_{i-1/2}^p = \alpha_{i-1/2}^p \phi\left(\theta_{i-1/2}^p\right), \tag{6.50}$$

where

$$\theta_{i-1/2}^p = \frac{\alpha_{I-1/2}^p}{\alpha_{i-1/2}^p} \qquad \text{with } I = \begin{cases} i-1 & \text{if } \lambda^p > 0, \\ i+1 & \text{if } \lambda^p < 0, \end{cases} \tag{6.51}$$

and ϕ is one of the limiter functions of Section 6.11. The flux function for the flux-limiter method is then

$$F_{i-1/2} = A^+ Q_{i-1} + A^- Q_i + \tilde{F}_{i-1/2}, \tag{6.52}$$

where the first term is the upwind flux and the correction flux $\tilde{F}_{i-1/2}$ is defined by

$$\tilde{F}_{i-1/2} = \frac{1}{2}|A|\left(1 - \frac{\Delta t}{\Delta x}|A|\right)\sum_{p=1}^{m}\tilde{\alpha}_{i-1/2}^p r^p. \tag{6.53}$$

Note that in the case of a scalar equation, we can take $r^1 = 1$ as the eigenvector of $A = \bar{u}$, so that $\Delta Q_{i-1/2} = \alpha_{i-1/2}^1$, which is what we called $\delta_{i-1/2}$ in Section 6.11. The formula (6.52) then reduces to (6.32). Also note that the flux $\tilde{F}_{i-1/2}$ (and hence $F_{i-1/2}$) depends not only on Q_{i-1} and Q_i, but also on Q_{i-2} and Q_{i+1} in general, because neighboring jumps are used in defining the limited values $\tilde{\alpha}_{i-1/2}^p$ in (6.50). The flux-limiter method thus has a five-point stencil rather than the three-point stencil of the Lax–Wendroff. This is particularly important in specifying boundary conditions (see Chapter 7). Note that this widening of the stencil gives a relaxation of the CFL restriction on the time step. For a five-point method the CFL condition requires only that the Courant number be less than 2. However, the CFL condition gives only a necessary condition on stability, and in fact these high-resolution methods are generally *not* stable for Courant numbers between 1 and 2. The larger stencil does not lead to a greater stability limit because the additional information is used only to limit the second-order correction terms.

Note that $|A|r^p = |\lambda^p| r^p$, so that (6.53) may be rewritten as

$$\tilde{F}_{i-1/2} = \frac{1}{2}\sum_{p=1}^{m}|\lambda^p|\left(1 - \frac{\Delta t}{\Delta x}|\lambda^p|\right)\tilde{\alpha}_{i-1/2}^p r^p. \tag{6.54}$$

This method for a system of equations can also be viewed as a *slope-limiter* method, if we think of $(Q_i - Q_{i-1})/\Delta x$ as approximating the slope vector, with each element giving an approximation to the slope for the corresponding element of q in a piecewise linear reconstruction. One might be tempted to limit the slope for each element of the vector separately, but in fact it is much better to proceed as above and limit the eigencoefficients obtained when the slope vector is expanded in eigenvectors of A. As a result, each wave is limited independently of other families, and the accuracy of smooth waves is not adversely affected by limiters being applied to other waves that may not be smooth.

For these wave-propagation algorithms it is perhaps most natural to view the limiter function as being a *wave limiter* rather than a slope limiter or flux limiter, since it is really the individual waves that are being limited after solving the Riemann problem. This viewpoint carries over naturally to nonlinear systems as introduced in Section 6.15 and explored more fully in Chapter 15. In the more general context, it is natural to use the notation

$$\tilde{\mathcal{W}}^p_{i-1/2} = \tilde{\alpha}^p_{i-1/2} r^p \tag{6.55}$$

to denote the limited wave appearing in (6.54).

6.14 Implementation

For the constant-coefficient linear system, we could compute the matrices A^+, A^-, and $|A|$ once and for all and compute the fluxes directly from the formulas given above. However, with limiters we must solve the Riemann problem at each interface to obtain a decomposition of $\Delta Q_{i-1/2}$ into waves $\alpha^p_{i-1/2} r^p$ and wave speeds λ^p, and these can be used directly in the computation of Q^{n+1}_i without ever forming the matrices. This approach also generalizes directly to nonlinear systems of conservation laws, where we do not have a single matrix A, but can still solve a Riemann problem at each interface for waves and wave speeds. This generalization is discussed briefly in the next section.

To accomplish this most easily, note that if we use the flux (6.52) in the flux-differencing formula (4.4) and then rearrange the upwind terms, we can write the formula for Q^{n+1}_i as

$$Q^{n+1}_i = Q_i - \frac{\Delta t}{\Delta x}\left(A^+ \Delta Q_{i-1/2} + A^- \Delta Q_{i+1/2}\right) - \frac{\Delta t}{\Delta x}\left(\tilde{F}_{i+1/2} - \tilde{F}_{i-1/2}\right),$$

where we drop the superscript n from the current time step because we will need to use superscript p below to denote the wave family. Each of the terms in this expression can be written in terms of the waves $\mathcal{W}^p_{i-1/2} = \alpha^p_{i-1/2} r^p$ and wave speeds λ^p:

$$\begin{aligned}
A^+ \Delta Q_{i-1/2} &= \sum_{p=1}^{m} (\lambda^p)^+ \mathcal{W}^p_{i-1/2}, \\
A^- \Delta Q_{i-1/2} &= \sum_{p=1}^{m} (\lambda^p)^- \mathcal{W}^p_{i-1/2}, \\
\tilde{F}_{i-1/2} &= \frac{1}{2} \sum_{p=1}^{m} |\lambda^p| \left(1 - \frac{\Delta t}{\Delta x} |\lambda^p|\right) \tilde{\mathcal{W}}^p_{i-1/2}.
\end{aligned} \tag{6.56}$$

6.15 Extension to Nonlinear Systems

The full extension of these methods to nonlinear problems will be discussed in Chapter 15 after developing the theory of nonlinear equations. However, the main idea is easily explained as a simple extension of what has been done for linear systems. Given states Q_{i-1} and Q_i, the solution to the Riemann problem will be seen to yield a set of waves $\mathcal{W}^p_{i-1/2} \in \mathbb{R}^m$ and speeds $s^p_{i-1/2} \in \mathbb{R}$, analogous to the linear problem, though now the speeds will vary with i, and so will the directions of the vectors $\mathcal{W}^p_{i-1/2}$ in phase space; they will no longer all be scalar multiples of a single set of eigenvectors r^p.

The quantities $A^+\Delta Q_{i-1/2}$ and $A^-\Delta Q_{i-1/2}$ have been generalized to *fluctuations* in Chapter 4, denoted by $\mathcal{A}^+\Delta Q_{i-1/2}$ and $\mathcal{A}^-\Delta Q_{i-1/2}$, with the property that

$$\mathcal{A}^-\Delta Q_{i-1/2} + \mathcal{A}^+\Delta Q_{i-1/2} = f(Q_i) - f(Q_{i-1}). \tag{6.57}$$

Note that for the linear case $f(Q_i) - f(Q_{i-1}) = A\Delta Q_{i-1/2}$, and this property is satisfied. In general we can think of setting

$$\begin{aligned} \mathcal{A}^-\Delta Q_{i-1/2} &= \sum_{p=1}^m \left(s^p_{i-1/2}\right)^- \mathcal{W}^p_{i-1/2}, \\ \mathcal{A}^+\Delta Q_{i-1/2} &= \sum_{p=1}^m \left(s^p_{i-1/2}\right)^+ \mathcal{W}^p_{i-1/2}, \end{aligned} \tag{6.58}$$

a direct extension of (6.56). There are, however, some issues concerned with rarefaction waves and entropy conditions that make the nonlinear case more subtle, and the proper specification of these flux differences will be discussed later. Once the waves, speeds, and flux differences have been suitably defined, the algorithm is virtually identical with what has already been defined in the linear case. We set

$$Q^{n+1}_i = Q^n_i - \frac{\Delta t}{\Delta x}\left(\mathcal{A}^-\Delta Q_{i+1/2} + \mathcal{A}^+\Delta Q_{i-1/2}\right) - \frac{\Delta t}{\Delta x}\left(\tilde{F}_{i+1/2} - \tilde{F}_{i-1/2}\right), \tag{6.59}$$

where

$$\tilde{F}_{i-1/2} = \frac{1}{2}\sum_{p=1}^m \left|s^p_{i-1/2}\right|\left(1 - \frac{\Delta t}{\Delta x}\left|s^p_{i-1/2}\right|\right)\widetilde{\mathcal{W}}^p_{i-1/2}. \tag{6.60}$$

Here $\widetilde{\mathcal{W}}^p_{i-1/2}$ represents a limited version of the wave $\mathcal{W}^p_{i-1/2}$, obtained by comparing this jump with the jump $\mathcal{W}^p_{I-1/2}$ in the same family at the neighboring Riemann problem in the upwind direction, so

$$I = \begin{cases} i-1 & \text{if } s^p_{i-1/2} > 0, \\ i+1 & \text{if } s^p_{i-1/2} < 0. \end{cases} \tag{6.61}$$

This limiting procedure is slightly more complicated than in the constant-coefficient case, in that $\mathcal{W}^p_{i-1/2}$ and $\mathcal{W}^p_{I-1/2}$ are in general no longer scalar multiples of the same vector r^p. So we cannot simply apply the scalar limiter function $\phi(\theta)$ to the ratio of these scalar coefficients as in the constant-coefficient linear case. Instead we can, for example, project

the vector $\mathcal{W}^p_{I-1/2}$ onto $\mathcal{W}^p_{i-1/2}$ and compare the length of this projection with the length of $\mathcal{W}^p_{i-1/2}$. This same issue arises for variable-coefficient linear systems and is discussed in Section 9.13.

When no limiting is used, this method is formally second-order accurate provided certain conditions are satisfied by the Riemann solution used; see Section 15.6. The methods generally perform much better, however, when limiters are applied.

6.16 Capacity-Form Differencing

In many applications the system of conservation laws to be solved most naturally takes the form

$$\kappa(x)q_t + f(q)_x = 0, \tag{6.62}$$

where $\kappa(x)$ is a spatially varying capacity function as introduced in Section 2.4. In the remainder of this chapter we will see how to extend the high-resolution methods defined above to this situation. In particular, this allows us to extend the methods to nonuniform grids as we do in Section 6.17. This material can be skipped without loss of continuity.

The equation (6.62) generally arises from an integral conservation law of the form

$$\frac{d}{dt}\int_{x_1}^{x_2} \kappa(x)q(x,t)\,dx = f(q(x_1,t)) - f(q(x_2,t)), \tag{6.63}$$

in which $\kappa(x)q(x,t)$ is the conserved quantity while the flux at a point depends most naturally on the value of q itself. It may then be most natural to solve Riemann problems corresponding to the flux function $f(q)$, i.e., by solving the equation

$$q_t + f(q)_x = 0 \tag{6.64}$$

locally at each cell interface, and then use the resulting wave structure to update the solution to (6.62). This suggests a method of the form

$$\kappa_i Q_i^{n+1} = \kappa_i Q_i^n - \frac{\Delta t}{\Delta x}\big[\mathcal{F}\big(Q_i^n, Q_{i+1}^n\big) - \mathcal{F}\big(Q_{i-1}^n, Q_i^n\big)\big]. \tag{6.65}$$

Dividing by κ_i gives

$$Q_i^{n+1} = Q_i^n - \frac{k}{\kappa_i \Delta x}\big[\mathcal{F}\big(Q_i^n, Q_{i+1}^n\big) - \mathcal{F}\big(Q_{i-1}^n, Q_i^n\big)\big]. \tag{6.66}$$

The form of equation (6.66) will be called *capacity-form differencing*. It is a generalization of conservation-form differencing to include the capacity function. The factor $\kappa_i \Delta x$ appearing in (6.66) has a natural interpretation as the effective volume of the ith grid cell if we think of κ_i as a fraction of the volume available to the fluid (as in porous-media flow, for example). Note that the updating formula (6.66) has the advantage of being conservative in the proper manner for the conservation law (6.63), since computing

$$\Delta x \sum_i \kappa_i Q_i^{n+1} = \Delta x \sum_i \kappa_i Q_i^n + \text{boundary fluxes}$$

from (6.65) shows that all the fluxes cancel except at the boundaries, where the boundary conditions must come into play.

We can rewrite the method (6.66) in the framework of the high-resolution wave-propagation algorithm as

$$Q_i^{n+1} = Q_i^n - \frac{\Delta t}{\kappa_i \Delta x}\left(\mathcal{A}^+ \Delta Q_{i-1/2}^n + \mathcal{A}^- \Delta Q_{i+1/2}^n\right) - \frac{\Delta t}{\kappa_i \Delta x}\left(\tilde{F}_{i+1/2}^n - \tilde{F}_{i-1/2}^n\right), \quad (6.67)$$

where as usual $\mathcal{A}^{\pm}\Delta Q_{i-1/2}$ are the fluctuations and $\tilde{F}_{i-1/2}$ is the correction flux based on the Riemann solution for (6.64) at the interface $x_{i-1/2}$. We now use the correction flux

$$\tilde{F}_{i-1/2} = \frac{1}{2}\sum_{p=1}^{M_w}\left(1 - \frac{\Delta t}{\kappa_{i-1/2}\Delta x}\left|s_{i-1/2}^p\right|\right)\left|s_{i-1/2}^p\right|\,\widetilde{\mathcal{W}}_{i-1/2}^p. \quad (6.68)$$

This is the general form for a system of m equations with M_w waves, as introduced in Section 6.15. The wave $\widetilde{\mathcal{W}}_{i-1/2}^p$ is a limited version of the wave $\mathcal{W}_{i-1/2}^p$, just as before, and these waves again are obtained by solving the Riemann problem for (6.64), ignoring the capacity function. The only modification from the formula for $\tilde{F}_{i-1/2}$ given in (6.60) is that Δx is replaced by $\kappa_{i-1/2}\Delta x$, where

$$\kappa_{i-1/2} = \frac{1}{2}(\kappa_{i-1} + \kappa_i). \quad (6.69)$$

Clearly, replacing Δx by some form of $\kappa\Delta x$ is necessary on the basis of dimensional arguments. If $\kappa(x)$ is smoothly varying, then using either $\kappa_{i-1}\Delta x$ or $\kappa_i\,\Delta x$ would also work, and the resulting method is second-order accurate for smooth solutions with any of these choices.

The choice $\kappa_{i-1/2}$ seems most reasonable, however, since the flux $\tilde{F}_{i-1/2}$ is associated with the interface between cells $\mathcal{C}_{i-1}$ and $\mathcal{C}_i$, rather than with either of the two cells. This term in the correction flux gives an approximation to the $\frac{1}{2}\Delta t^2 q_{tt}$ term in the Taylor series expansion once it is inserted in the flux-differencing term of (6.67). We compute, for smooth solutions, that

$$q_{tt} = \frac{1}{\kappa}\left(\frac{1}{\kappa}[f'(q)]^2 q_x\right)_x,$$

and centering of these terms again suggests that the inner $1/\kappa$ should be evaluated at $x_{i\pm1/2}$. In Section 6.17.1, where nonuniform grids are discussed, we will see that this choice makes clear physical sense in that case, and is correct even if κ is not smoothly varying.

6.17 Nonuniform Grids

One natural example of a capacity function arises if we solve a standard conservation law $q_t + f(q)_x = 0$ on a nonuniform grid such as shown on the right of Figure 6.7. There are two philosophically different approaches that could be taken to derive a numerical method on this grid:

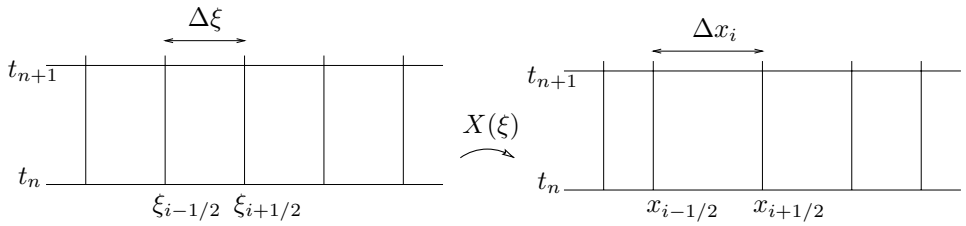

Fig. 6.7. The grid mapping $X(\xi)$ maps a uniform computational grid in ξ–t space (on the left) to the nonuniform x–t grid in physical space (on the right).

1. Work directly in the *physical space* (the right side of Figure 6.7), and derive a finite volume method on the nonuniform gird for the integral form of the conservation law on the physical-grid cells.
2. View the nonuniform grid as resulting from some coordinate mapping applied to a uniform grid in *computational space*. Such a grid is illustrated on the left side of Figure 6.7, where $\Delta\xi$ is constant and the mapping function $X(\xi)$ defines $x_{i-1/2} = X(\xi_{i-1/2})$. If we can transform the equation in x and t to an equivalent equation in ξ and t, then we can solve the transformed equation on the uniform grid.

The first approach is generally easier to use in developing finite volume methods for conservation laws, for several reasons:

- The transformed equation in computational space includes *metric terms* involving $X'(\xi)$, as we will see below. The mapping must be smooth in order to achieve good accuracy if we attempt to discretize the transformed equations directly. In practice we might want to use a highly nonuniform grid corresponding to a nonsmooth function $X(\xi)$.
- Even if $X(\xi)$ is smooth, it may not be easy to discretize the transformed equation in ξ in a way that exactly conserves the correct physical quantities in x. By contrast, a finite volume method in the physical space automatically achieves this if we write it in terms of fluxes at the cell edges.
- Using a Godunov-type method requires solving a Riemann problem at each cell interface, and the transformed equations lead to a transformed Riemann problem. It is often simpler to solve the original, physically meaningful Riemann problem in x.

For these reasons we will derive finite volume methods in the physical domain. However, once the method has been derived, we will see that we can then view it as a discretization of the transformed equation. This viewpoint is useful in implementing the methods, as we can then express the method as a finite volume method with a capacity function applied on the uniform ξ-grid. As we will see, the capacity κ_i of the ith grid cell $[\xi_{i-1/2}, \xi_{i+1/2}]$ is then the ratio of the physical cell length $\Delta x_i \equiv (x_{i+1/2} - x_{i-1/2})$ to $\Delta\xi$, which is a natural measure of the capacity of the computational cell. For a smooth mapping $X(\xi)$ this can be viewed as an approximation to the capacity function $\kappa(x) \equiv X'(\xi)$, the Jacobian of the mapping, but the finite volume method remains valid and accurate even if the mapping is not smooth.

In Chapter 23, we will see that this approach extends naturally to quadrilateral grids in more than one space dimension. Again we will derive finite volume methods in the

irregular physical grid cells, but implement the methods using capacity-form differencing on a uniform rectangular grid.

We now derive a finite volume method in the physical domain. We have

$$\begin{aligned}\int_{x_{i-1/2}}^{x_{i+1/2}} q(x,t_{n+1})\,dx &= \int_{x_{i-1/2}}^{x_{i+1/2}} q(x,t_n)\,dx \\ &\quad - \left(\int_{t_n}^{t_{n+1}} f\big(q\big(x_{i+1/2},t\big)\big)\,dt - \int_{t_n}^{t_{n+1}} f\big(q\big(x_{i-1/2},t\big)\big)\,dt\right),\end{aligned} \tag{6.70}$$

which suggests the finite volume method

$$Q_i^{n+1} = Q_i^n - \frac{\Delta t}{\Delta x_i}\big[\mathcal{F}\big(Q_i^n, Q_{i+1}^n\big) - \mathcal{F}\big(Q_{i-1}^n, Q_i^n\big)\big], \tag{6.71}$$

where $\Delta x_i = x_{i+1/2} - x_{i-1/2}$ is the width of the ith cell and

$$Q_i^n \approx \frac{1}{\Delta x_i}\int_{x_{i-1/2}}^{x_{i+1/2}} q(x,t_n)\,dx.$$

The numerical flux $\mathcal{F}(Q_{i-1}^n, Q_i^n)$ should be, as usual, an approximation to

$$\frac{1}{\Delta t}\int_{t_n}^{t_{n+1}} f\big(q\big(x_{i-1/2},t\big)\big)\,dt.$$

For Godunov's method, this is determined simply by solving the Riemann problem and evaluating the flux along $x/t = 0$. The fact that the grid is nonuniform is immaterial in computing the Godunov flux. The nonuniformity of the grid does come into the second-order correction terms, however, since approximating the slopes q_x with cell values requires paying attention to the grid spacing. This is discussed in Section 6.17.1.

Next we will see that the method (6.71) can be reinterpreted as a method on the uniform computational grid. Let

$$\kappa_i = \Delta x_i/\Delta\xi,$$

where $\Delta\xi$ is the uniform cell size in the computational grid shown on the left in Figure 6.7. Then the method (6.71) can be written as

$$Q_i^{n+1} = Q_i^n - \frac{\Delta t}{\kappa_i\Delta\xi}\big[\mathcal{F}\big(Q_i^n, Q_{i+1}^n\big) - \mathcal{F}\big(Q_{i-1}^n, Q_i^n\big)\big]. \tag{6.72}$$

Let

$$\bar q(\xi,t) = q(X(\xi),t).$$

If we now assume that the coordinate mapping $X(\xi)$ is differentiable, then the change of variables $x = X(\xi)$, for which $dx = X'(\xi)\,d\xi$, gives

$$\begin{aligned}\int_{x_{i-1/2}}^{x_{i+1/2}} q(x,t)\,dx &= \int_{\xi_{i-1/2}}^{\xi_{i+1/2}} q(X(\xi),t)\,X'(\xi)\,d\xi \\ &= \int_{\xi_{i-1/2}}^{\xi_{i+1/2}} \bar q(\xi,t)\kappa(\xi)\,d\xi,\end{aligned}$$

where the capacity function $\kappa(\xi)$ is the Jacobian $X'(\xi)$, as expected. Hence the conservation law

$$\frac{d}{dt}\int_{x_{i-1/2}}^{x_{i+1/2}} q(x,t)\,dx = f\big(q\big(x_{i-1/2},t\big)\big) - f\big(q\big(x_{i+1/2},t\big)\big)$$

is transformed into

$$\frac{d}{dt}\int_{\xi_{i-1/2}}^{\xi_{i+1/2}} \bar{q}(\xi,t)\kappa(\xi)\,d\xi = f\big(\bar{q}\big(\xi_{i-1/2},t\big)\big) - f\big(\bar{q}\big(\xi_{i+1/2},t\big)\big).$$

This has the form of the integral conservation law (6.63) in the computational domain. The finite volume method (6.71), when rewritten as (6.72), can be viewed as a capacity-form differencing method on the uniform ξ-grid.

We can also interpret Q_i^n as an approximation to a cell average of $\bar{q}$ over the computational domain:

$$\begin{aligned} Q_i^n &\approx \frac{1}{\Delta x_i}\int_{x_{i-1/2}}^{x_{i+1/2}} q(x,t_n)\,dx \\ &= \frac{1}{\kappa_i\,\Delta\xi}\int_{\xi_{i-1/2}}^{\xi_{i+1/2}} \bar{q}(\xi,t_n)\kappa(\xi)\,d\xi \\ &\approx \frac{1}{\Delta\xi}\int_{\xi_{i-1/2}}^{\xi_{i+1/2}} \bar{q}(\xi,t_n)\,d\xi. \end{aligned} \tag{6.73}$$

6.17.1 High-Resolution Corrections

One way to derive high-resolution methods for the advection equation $q_t + \bar{u}q_x = 0$ (with $\bar{u} > 0$, say) on a nonuniform grid is to use the REA algorithm approach from Section 6.4, which is easily extended to nonuniform grids. Given cell averages, we reconstruct a piecewise linear function on each of the grid cells, evolve the advection equation exactly by shifting this function over a distance $\bar{u}\,\Delta t$, and average onto the grid cells to obtain new cell averages. If the slopes are all chosen to be $\sigma_i^n = 0$, then this reduces to the upwind method

$$Q_i^{n+1} = Q_i^n - \frac{\bar{u}\,\Delta t}{\kappa_i\,\Delta\xi}\big(Q_i^n - Q_{i-1}^n\big),$$

which has the form (6.72) with $\mathcal{F}(Q_{i-1}^n, Q_i^n) = \bar{u}\,Q_{i-1}^n$. With nonzero slopes we obtain

$$\begin{aligned} Q_i^{n+1} = Q_i^n &- \frac{\bar{u}\,\Delta t}{\kappa_i\,\Delta\xi}\big(Q_i^n - Q_{i-1}^n\big) \\ &- \frac{1}{2}\frac{\bar{u}\,\Delta t}{\kappa_i\,\Delta\xi}\big[(\kappa_i\,\Delta\xi - \bar{u}\,\Delta t)\sigma_i^n - (\kappa_{i-1}\,\Delta\xi - \bar{u}\,\Delta t)\sigma_{i-1}^n\big]. \end{aligned} \tag{6.74}$$

Recall that on a uniform grid the Lax–Wendroff method is obtained by taking slopes $\sigma_{i-1}^n = (Q_i^n - Q_{i-1}^n)/\Delta x$. On a nonuniform grid the distance between cell centers is

$\kappa_{i-1/2}\,\Delta\xi$, where $\kappa_{i-1/2} = \frac{1}{2}(\kappa_{i-1} + \kappa_i)$, and the natural generalization of the Lax–Wendroff method is obtained by setting

$$\sigma_{i-1}^n = \frac{Q_i^n - Q_{i-1}^n}{\kappa_{i-1/2}\,\Delta\xi}. \tag{6.75}$$

This corresponds to a correction flux

$$\tilde{F}_{i-1/2} = \frac{1}{2}\left(\frac{\kappa_{i-1}}{\kappa_{i-1/2}} - \frac{\bar{u}\,\Delta t}{\kappa_{i-1/2}\,\Delta\xi}\right)\bar{u}\big(Q_i^n - Q_{i-1}^n\big). \tag{6.76}$$

The natural generalization of this to systems of equations gives a correction flux similar to (6.68) but with the 1 replaced by $\kappa_i/\kappa_{i-1/2}$:

$$\tilde{F}_{i-1/2} = \frac{1}{2}\sum_{p=1}^{M_w}\left(\frac{\kappa_{i-1}}{\kappa_{i-1/2}} - \frac{\Delta t}{\kappa_{i-1/2}\,\Delta\xi}\big|s_{i-1/2}^p\big|\right)\big|s_{i-1/2}^p\big|\,\widetilde{\mathcal{W}}_{i-1/2}^p. \tag{6.77}$$

For smooth κ this is essentially the same as (6.68), but for nonsmooth κ (6.77) might give better accuracy.

Exercises

6.1. Verify that (6.13) results from integrating the piecewise linear solution $\tilde{q}^n(x, t_{n+1})$.

6.2. Compute the total variation of the functions

(a)

$$q(x) = \begin{cases} 1 & \text{if } x < 0, \\ \sin(\pi x) & \text{if } 0 \le x \le 3, \\ 2 & \text{if } x > 3, \end{cases}$$

(b)

$$q(x) = \begin{cases} 1 & \text{if } x < 0 \text{ or } x = 3, \\ 1 & \text{if } 0 \le x \le 1 \text{ or } 2 \le x < 3, \\ -1 & \text{if } 1 < x < 2, \\ 2 & \text{if } x > 3. \end{cases}$$

6.3. Show that any TVD method is monotonicity-preserving. (But note that the converse is not necessarily true: a monotonicity-preserving method may not be TVD on more general data.)

6.4. Show that (6.25) is valid by showing that, for any function $q(x)$, if we define discrete values Q_i by averaging $q(x)$ over grid cells, then $\mathrm{TV}(Q) \le \mathrm{TV}(q)$. Hint: Use the definition (6.19) and the fact that the average value of q lies between the maximum and minimum values on each grid cell.

6.5. Show that the *minmod* slope guarantees that (6.23) will be satisfied in general, and hence the *minmod* method is TVD.

6.6. Show that taking

$$\delta^n_{i-1/2} = Q^n_i - Q^n_{i-1}$$

in (6.32) corresponds to using the downwind slope for σ in both cases $\bar{u} > 0$ and $\bar{u} < 0$, and that the resulting flux gives the Lax–Wendroff method.

6.7. Show that if $\bar{u} < 0$ we can apply Theorem 6.1 to the flux-limiter method (6.41) by choosing

$$C^n_{i-1} = 0,$$
$$D^n_i = -\nu + \frac{1}{2}\nu(1+\nu)\left(\phi\left(\theta^n_{i-1/2}\right) - \frac{\phi\left(\theta^n_{i+1/2}\right)}{\theta^n_{i+1/2}}\right)$$

in order to show that the method is TVD provided $-1 \le \nu \le 0$ and the bound (6.44) holds. Hence the same restrictions on limiter functions are found in this case as discussed in Section 6.12.

6.8. Verify that (6.47) is required for symmetry.

6.9. Verify that (6.48) and (6.49) are equivalent and yield the Lax–Wendroff method.

6.10. Plot the van Leer limiter from (6.39b), and verify that it lies in the Sweby region shown in Figure 6.6.